

Outer-magnetospheric model for Vela-like pulsars: Formation of sub-GeV spectrum

J. Takata,^{1*} S. Shibata,² K. Hirotani,³

¹*Graduate School of Science and Engineering, Yamagata University, Yamagata 990-8560, Japan*

²*Department of Physics, Yamagata University, Yamagata 990-8560, Japan*

³*Max-Planck-Institut fuer Kernphysik, Postfach 103980 D-69029 Heidelberg, Germany*

Released 2003 Xxxxx XX

ABSTRACT

We investigate the γ -ray emission from a outer-gap accelerator, which is located in the outer-magnetosphere of a pulsar. The charge depletion from the Goldreich-Julian density causes a large electric field along the magnetic field lines. The electric field accelerates electrons and positrons to high energies. We solve the formation of the electric field self-consistently with the radiation and the pair-creation processes in one-dimensional geometry along the magnetic field lines, and calculate curvature spectrum to compare with the observations.

We find that because the particles escape from the accelerating region with large Lorentz factors as $10^{7.5}$, curvature radiation from the outside of the gap, in which there is no electric field, still has a important contribution to the spectrum. Including the outside emission, the model spectra are improved between 100 MeV and 1 GeV for the Vela-type pulsars. Since the field line curvature close to the light cylinder affects the spectrum in several hundred MeV, there is a possibility to diagnose the field structure by using the spectrum in these bands. The difference found in the γ -ray spectra of the twin pulsars, PSR B0833-45 (Vela) and B1706-44, is deduced from the dimensionless electric current running through the gap. The extension to the three-dimensional modeling with self-consistent electrodynamics is necessary to understand the difference in the observed flux between the twin pulsars.

Key words: gamma-rays: theory – pulsars: individual (Vela pulsar, PSR B1706-44).

1 INTRODUCTION

The *Compton Gamma Ray Observatory* had detected seven γ -ray pulsars (Thompson et al. 1999). The observed light curves and energy spectra tell about the energy of accelerated particles and the geometry of γ -ray emission regions in the pulsar magnetosphere. These observations provide constraints on proposed radiation models. The next-generation γ -ray space telescopes and ground based Čerenkov telescopes are expected to provide further constraints on the models.

A pulsation in γ -rays implies that the acceleration of particles and the subsequent radiation occur within the light cylinder, of which axial distance is given by $\varpi_{lc} = c/\Omega$, where Ω is angular frequency of the star, and c the speed of light.

The charge depletion from Goldreich-Julian charge density causes a large electric field E_{\parallel} along the magnetic field lines. The Goldreich-Julian density is given by (Goldreich & Julian 1969, here after GJ)

$$\rho_{GJ} = -\frac{\Omega B_z}{2\pi c} \frac{1}{[1 - (\Omega\varpi/c)^2]}, \quad (1)$$

where B_z is the component of the magnetic field along the rotation axis, and ϖ the axial distance. A potential drop in such a charge depletion region (gap) is only a small fraction of the available electromotive force exerted on the spinning neutron star surface. The γ -ray emissions in the pulsar magnetosphere have been argued with polar-cap model (e.g. Sturrock 1971; Ruderman & Sutherland 1975) and outer-gap model (e.g. Cheng, Ho & Ruderman 1986a, b); each acceleration region is located near stellar surface above the magnetic poles and in the outer-magnetosphere around the null charge surface ($B_z = 0$) above the last-open field line, respectively.

After Cheng et al. (1986a,b), the outer-gap model has been studied in two different pictures. In the first picture, the observed light curves have been studied in an effort to construct the three-dimensional models for the outer-gap (Romani & Yadigaroglu 1995; Romani 1996; Cheng, Ruderman & Zhang 2000). The peaks in the light curves are interpreted as an effect of aberration and time delay for emitted photons, thereby the outer-gap model has been successful in explaining the double peaks in one period and phase separation of the pulses in different energies from the radio to γ -ray. The observed phase resolved spectra have also been calculated with the models, in which pair cascade process has been solved with

assumed field-aligned electric field E_{\parallel} . The predicted phase resolved spectrum depends on the assumption of the strength and distribution of E_{\parallel} . Thus, the models are not satisfactory in the sense of electrodynamics.

The other approach has focused on electrodynamics in the outer-gap. Cheng et al. (1986a) discussed the electric structure in the vacuum gap. They gave a solution for the Poisson equation with rectilinear geometry. Hirotani & Shibata (1999, hereafter HS) proposed a non-vacuum electrodynamic model for the outer-gap. Although they worked on only one dimension along the last-open field line, they solved the accelerating electric field self-consistently with curvature radiation and pair-creation processes. Although the calculated γ -ray spectra were consistent with the EGRET observation in the GeV band, there were much harder than what is observed below 1 GeV.

In this paper, to improve the HS model, we take account of the curvature radiation from the outside of the gap. Even though the electric field is screened out in this region, particles still possess sufficient energy and hence contribute to the γ -ray luminosity between 100 MeV and 1 GeV. Quite recently, Hirotani, Harding & Shibata (2003) presented a model in which particle motion is precisely solved under the electric force and radiation reaction force (see also Hirotani 2003 for a review). Although they also took account of the radiation from the outside of the gap, we treat this effect in some detail by considering non-dipole field near the light cylinder because the field line are expected to deviate from dipole configuration by the influence of the pulsar wind or the electric current. Then, we show that the position of low energy cut-off in the curvature spectrum depends on the curvature radius of the field lines near the light cylinder. In applying our model, we consider the twin pulsars, PSR B0833-45 (Vela) and B1706-44. It is remarkable that these pulsars show distinctive γ -ray spectra even though they have very similar magnetospheric parameters as well as surface temperatures (Gotthelf, Halpern & Dodson 2002). Thus this pair of pulsars gives unique opportunity to examine the model capability. We shall show that the difference of spectral peak energy between the two, about 3 GeV for Vela and about 1 GeV for B1706-44, is understood well with the present model. On the other hand, we elucidate limitations of one-dimensional approximation.

In §2 we describe the basic equations for the electrodynamics in the gap. In §3 we discuss the curvature radiation from the outside of the gap. In §4 we apply our model to the Vela pulsar and PSR B1706-44. The necessity for the three-dimensional electrodynamic model is discussed in §5.

2 ONE DIMENSIONAL OUTER-GAP MODEL

In this section, we present the basic equations to describe the electrodynamics in the gap, after HS. We give the Poisson equation for the acceleration field (§§2.1), the continuity equations for particles and γ -rays (§§2.2). We impose the boundary conditions in §§2.3 and finally describe the X -ray field in §§2.4

2.1 Poisson equation

If the magnetosphere is corotating with the star, an electric field,

$$\mathbf{E} = -\frac{(\boldsymbol{\Omega} \times \mathbf{r}) \times \mathbf{B}}{c} \equiv -\nabla\Phi_{co}, \quad (2)$$

which is perpendicular to the magnetic field \mathbf{B} , is exerted at position \mathbf{r} . The corotational potential Φ_{co} satisfies the Poisson equation

$$\nabla^2\Phi_{co} = -4\pi\rho_{GJ}. \quad (3)$$

Meanwhile in the gap, since the real charge density ρ deviates from ρ_{GJ} , the electrostatic potential Φ differs from Φ_{co} . The difference is extracted as the *non-corotational* potential, $\Phi_{nco} = \Phi - \Phi_{co}$. The Poisson equation, $\nabla^2\Phi = -4\pi\rho$, yields

$$\nabla^2\Phi_{nco} = -4\pi\rho_{eff}, \quad (4)$$

where $\rho_{eff} = \rho - \rho_{GJ}$ is the effective charge density which produces the field-aligned electric field, $E_{||} = -\mathbf{B} \cdot \nabla\Phi_{nco}/|\mathbf{B}|$.

If the gap width $W_{||}$ along the magnetic field lines is much shorter than the curvature radius ($\sim \varpi_{lc}$) of the field lines, we may assume that the field lines are straight in the gap. In §4, we shall see that $W_{||}$ is about 10 per cent of ϖ_{lc} . By assuming that the gap width is much smaller than the trans-field thickness of the gap, we rewrite equation (4) as

$$\begin{aligned} \frac{d^2\Phi_{nco}(s)}{ds^2} &= -4\pi[\rho(s) - \rho_{GJ}(s)] \\ &= -4\pi e \left[N_+(s) - N_-(s) - \frac{\rho_{GJ}(s)}{e} \right], \end{aligned} \quad (5)$$

where N_+ (N_-) is the positrons (electrons) number density, s is the arc length along the last-open field line from the surface, and $-e$ is the electron charge. The accelerating electric field is given by

$$E_{||}(s) = -\frac{d\Phi_{nco}}{ds}. \quad (6)$$

Unless the gap is close to the light cylinder, the GJ charge density (1) is approximated as

$$\rho_{GJ} \sim -\frac{\Omega B_z}{2\pi c}. \quad (7)$$

We use this expression for the GJ charge density.

2.2 Continuity equations for particles and γ -rays

As the Poisson equation (5) indicates, particle's distribution is needed to obtain the electric structure in the gap. If charged particles move along the magnetic field lines with the speed $\sim c$, the steady continuity equation without any particle sources yields

$$\frac{N_{\pm}(s)}{B(s)} = \text{constant along magnetic field line.} \quad (8)$$

However, γ -rays radiated by particles may convert into electron-positron pairs. In the outer-magnetosphere, $X\gamma \rightarrow e^-e^+$ process has a particular importance with X -ray illumination from the neutron star surface or the magnetosphere. Taking account of the pair-creation, we write down the continuity equation into the form,

$$\pm B \frac{d}{ds} \left(\frac{N_{\pm}}{B} \right) = \frac{1}{c \cos \Psi} \int_0^{\infty} d\epsilon_{\gamma} [\eta_{p+} G_+ + \eta_{p-} G_-], \quad (9)$$

where we assume that the electric field is positive in the gap for the definite of sign of polarity so that e^+ (or e^-) may be accelerated outward (or inward); $G_{p+}(s, \epsilon_{\gamma})$ (or G_{p-}) denotes the distribution function of outwardly (or inwardly) propagating γ -rays; ϵ_{γ} is the photon energy normalized by $m_e c^2$; Ψ is the angle between the particle's motion and the meridional plane and is assumed to be $\Psi = \sin^{-1}(r\Omega \sin \theta/c)$, where θ is the colatitude at the point considered. The pair-creation rate $\eta_{p\pm}(s, \epsilon_{\gamma})$ per unit time per γ -ray photon with ϵ_{γ} is written down as

$$\eta_{p\pm}(s, \epsilon_{\gamma}) = (1 - \mu_c) c \int_{\epsilon_{th}}^{\infty} d\epsilon_X \frac{dN_X}{d\epsilon_X} \sigma_p, \quad (10)$$

where $d\epsilon_X \cdot dN_X/d\epsilon_X$ is the X -ray number density between energies $m_e c^2 \epsilon_X$ and $m_e c^2 (\epsilon_X + d\epsilon_X)$, $\cos^{-1} \mu_c$ is the collision angle between a X -ray and a γ -ray, $m_e c^2 \epsilon_{th}$ is the threshold energy for the pair-creation, and σ_p is the pair-creation cross-section, which is given by

$$\sigma_p(\epsilon_{\gamma}, \epsilon_X) = \frac{3}{16} \sigma_T (1 - v^2) \left[(3 - v^4) \ln \frac{1 + v}{1 - v} - 2v(2 - v^2) \right], \quad (11)$$

$$v(\epsilon_{\gamma}, \epsilon_X) = \sqrt{1 - \frac{2}{1 - \mu_c} \frac{1}{\epsilon_{\gamma} \epsilon_X}},$$

where σ_T is the Thomson cross section.

Let us next consider the continuity equation for γ -rays. The γ -rays radiated by high energy particles are beamed nearly tangentially to the magnetic field. Although γ -rays deviate from the magnetic field line on which γ -rays were emitted, the one-dimensional approximation does not treat this effect correctly. We deal with γ -ray distribution along the magnetic field line. Then we can write down the continuity equation into the form,

$$\pm B(s) \frac{d}{ds} \left[\frac{G_{\pm}(s, \epsilon_{\gamma})}{B(s)} \right] = \frac{-\eta_{p\pm} G_{\pm}(s, \epsilon_{\gamma}) + \eta_c N_{\pm}(s)}{c \cos \Psi}, \quad (12)$$

where the first term of the right-hand side represents annihilation of γ -rays by the pair-creation, and the second term represents production by the curvature radiation. The emissivity for the curvature radiation η_c is given by

$$\eta_c(R_c, \Gamma, \epsilon_{\gamma}) = \frac{\sqrt{3}e^2}{hR_c} \frac{\Gamma}{\epsilon_{\gamma}} F\left(\frac{\epsilon_{\gamma}}{\epsilon_c}\right), \quad (13)$$

$$\epsilon_c = \frac{3}{4\pi} \frac{hc\Gamma^3}{m_e c^2 R_c}, \quad (14)$$

and

$$F(x) = x \int_x^{\infty} K_{5/3}(t) dt, \quad (15)$$

where R_c is the curvature radius of the magnetic field line, Γ is the Lorentz factor of particles, $K_{5/3}$ is the modified Bessel function of order 5/3, h is the Planck constant, and $m_e c^2 \epsilon_c$ gives the characteristic curvature photon energy radiated by a particle with Lorentz factor Γ . The Lorentz factor in the gap is obtained by assuming that the particle's motion immediately saturates in the balance between the electric and the radiation reaction forces,

$$\Gamma_{sat}(R_c, E_{||}) = \left(\frac{3R_c^2}{2e} E_{||} + 1 \right)^{1/4}. \quad (16)$$

The unity in the brackets in (16) does not influence Γ_{sat} in the gap except for near the boundaries, where $E_{||} = 0$.

Saturation simplifies the problem significantly, but requires a condition. The Γ_{sat} is the Lorentz factor at which the typical accelerating time t_{ac} equals the typical traditional damping time t_d of the particles. The particles whose Lorentz factor is larger than Γ_{sat} will be decelerated by the radiation back reaction because $t_d < t_{ac}$. On the other hand, the particles which have $\Gamma < \Gamma_{sat}$ in the gap will be accelerated because $t_d > t_{ac}$. If the two timescales are less than crossing time $t_{cr} = W_{||}/c$,

$$t_{cr} \gg t_{ac} \text{ and } t_{cr} \gg t_d, \quad (17)$$

then the particles in the gap will have the saturated Lorentz factor given by equation (16). As has been recently showed by Hirovani et al. (2003), in which motion of unsaturated particles are solved, the condition $t_{cr} \gg t_{ac}$ in (17) is not satisfied effectively for some pulsars and/or part of the gap. In the present application to the Vela-type pulsars, γ -rays producing the peak in the spectrum emerge from the central part of the gap, for which use of (16) provides a good approximation. However, emission near and the outside of the gap requires a different treatment, which is discussed in §3.

2.3 Boundary conditions

In this subsection, we give the boundary conditions to solve equations (5), (9), and (12).

The inner ($s = s_1$) and outer ($s = s_2$) boundaries are defined so that $E_{||}$ may vanish,

$$E_{||}(s_1) = E_{||}(s_2) = 0. \tag{18}$$

We assume that γ -rays do not come into the gap across either of the boundaries, that is,

$$G_+(s_1) = G_-(s_2) = 0. \tag{19}$$

Attempting to explain the activity of pulsars, it is generally believed that some currents circulate in the magnetosphere globally. Hence we permit particles to come into gap through the boundaries. We parameterize the inflows across the inner and the outer boundaries such that,

$$\frac{N_+(s_1)}{\Omega B(s_1)/2\pi c} = j_1, \quad \frac{N_-(s_2)}{\Omega B(s_2)/2\pi c} = j_2. \tag{20}$$

If $j_1 = 1$ (or $j_2 = 1$), particles are injected into the gap at the Goldreich-Julian rate at $s = s_1$ (or $s = s_2$). The particle's continuity equations (9) give the current conservation per unit flux tube,

$$j_{tot} \equiv \frac{N_+(s)}{\Omega B(s)/2\pi c} + \frac{N_-(s)}{\Omega B(s)/2\pi c} = \text{constant along } s. \tag{21}$$

By defining j_g as the amount of created current carriers per unit flux tube within the gap, the conservation law (21) yields

$$j_1 + j_2 + j_g = j_{tot}. \tag{22}$$

The global conditions, which include an interaction with the pulsar wind, should determine the current. In our local model, therefore, we adopt (j_{tot}, j_1, j_2) or (j_g, j_1, j_2) as the set of free model parameters.

We have the 7 boundary conditions (18) ~ (22) against the 5 unknown functions. This is

because $E_{||} = 0$ is imposed at both boundaries and because j_{tot} (or j_g) is externally imposed. In other words, we cannot impose the conditions $E_{||}(s_1) = 0$ and $E_{||}(s_2) = 0$ for arbitrary given boundaries s_1 and s_2 . By moving the boundaries step by step iteratively, we seek for the boundaries that satisfy the required conditions.

2.4 X-ray field in the magnetosphere

We need to know a soft photon field to calculate the pair-creation rate $\eta_{p\pm}$. For GeV γ -ray photons, which dominate in the curvature photons radiated in the gap, σ_p is maximized at the soft X-ray band. The observed X-rays are dominated by the surface blackbody radiation for the Vela-like pulsars, and by the non-thermal radiation for the Crab-like pulsars. In this paper, because we apply our model to the Vela-like pulsars (§4), we take only the surface blackbody radiation as the soft photon field.

For the blackbody case, the photon number density between energy $m_e c^2 \epsilon_X$ and $m_e c^2 (\epsilon_X + d\epsilon_X)$ is given by the Planck law,

$$\frac{dN_X}{d\epsilon_X} = \frac{1}{4\pi} \left(\frac{2\pi m_e c^2}{ch} \right)^3 \left(\frac{A_s}{4\pi r^2} \right) \frac{\epsilon_X^2}{\exp(m_e c^2 \epsilon_X / kT_s) - 1}, \quad (23)$$

where r is the radial distance from the centre of the star, A_s is the observed emitting area and kT_s refers to the surface temperature. We calculate the pair-creation rate (10) by using (23) at each point in the gap, where the collision angle μ_c is given by

$$\mu_c = \cos \phi_{\gamma X} \sin \theta, \quad (24)$$

with $\phi_{\gamma X} = \sin^{-1}(r \sin \theta \Omega / c)$.

3 CURVATURE RADIATION FROM THE OUTSIDE OF THE GAP

In the HS model, a self-consistent determination of the accelerating electric field is successful in reproducing the γ -ray spectrum in the GeV band, at which the pulsed radiation peaks in νF_ν diagram. However, the calculated spectrum deviates from the observed that in lower energy bands. This problem is solved by treating properly how particle energy evolve near and beyond the gap boundaries.

Because the saturated Lorentz factor Γ_{sat} given by (16) is proportional to $E_{||}^{1/4}$, Γ_{sat} does not change much in the gap, except for around boundaries. In such case, the curvature spectrum produced in the gap is similar to the spectrum that is emitted by mono-energetic

particles, and follows E_γ^{-p} with the photon index $p \sim 2/3$ below the cut-off energy E_c . However, observations indicate much soft slopes; $E_\gamma^{-1.3} - E_\gamma^{-1.6}$ in MeV band.

If one uses the saturated Lorentz factor given by equation (16), Γ_{sat} decreases near the inner and outer boundaries because $E_{||}$ decreases. It is notable that Γ_{sat} is the Lorentz factor at which $t_{ac} = t_d$. The time scales t_{ac} and t_d become longer near the boundaries as compared with the crossing time t_{cr} . In fact, the ratio of t_{cr} to t_d ,

$$\begin{aligned} \frac{t_d}{t_{cr}} &\sim \frac{3 m_e c^2 R_c^2}{2 e^2 \Gamma^3} \times W_{||}^{-1} \\ &= 4 \frac{0.1 \varpi_{lc}}{W_{||}} \left(\frac{\Omega}{100 \text{rads}^{-1}} \right)^{-1} \left(\frac{\Gamma}{10^7} \right)^{-3} \left(\frac{R_c}{0.5 \varpi_{lc}} \right)^2, \end{aligned} \quad (25)$$

is larger than unity near the boundaries. As a result, the Lorentz factor is kept greater than Γ_{sat} near and beyond the boundaries. These particles escape from the gap with a large Lorentz factor $\Gamma_{out} \sim a \text{ few times } 10^7$ and will radiate γ -rays even outside of the gap. The damping length after the escape should be comparable with or longer than the gap width $W_{||}$.

On these aspects, we take account of the radiation from the outside of the gap as well as that from inside. Although Hirovani et al. (2003) calculated Γ_{out} numerically by solving the unsaturated motion of particles in the gap, we shall estimate Γ_{out} semi-analytically; we assume that the particles are ejected from the gap with the Lorentz factor given by a saturated value at $t_{cr} = t_d$. On leaving the gap, particles simply lose their energy by radiation, because $E_{||}$ is screened out. The Lorentz factor of the particles ejected from the gap decreases as

$$\frac{d\Gamma(s)}{ds} = -\frac{2 e^2 \Gamma^4(s)}{3 m_e c^2 R_c^2(s)}. \quad (26)$$

The rate of decrease in Γ per unit length is proportional to $\Gamma^4(s)$ if $R_c = \text{const}$. Then, the spectrum of γ -rays from the outside of the gap is the same as the spectrum made by particles with an energy distribution of

$$\frac{dN_e(\Gamma)}{d\Gamma} \propto \Gamma^{-4}. \quad (27)$$

In short, we obtain a power-low γ -ray spectrum by superposing the curvature radiation at different positions; therefore, we need not assume a power energy distribution for particles to explain the observed power spectrum.

The curvature photons emitted by the particles obeying equation (27) exhibits a soft, power-low spectrum with a photon index around $p = 5/3$ for $E_\gamma < E_{out}$ where $E_{out} = (3h/4\pi)(\Gamma_{out}^3 c/R_c)$ is the critical energy for the highest-energy particles. The soft, power-low

spectrum will extend down to the energy $E_{min} = (3h/4\pi)(\Gamma_{min}^3 c/R_c)$, where Γ_{min} is the Lorentz factor below which the γ -rays are beamed out from the line of the sight due to the magnetic curvature, for instance. Below E_{min} , the curvature spectrum becomes hard with a photon index around $p = 2/3$. If we estimate E_{min} with the particles energy when they escape across the light cylinder, we obtain $E_{min} \sim 80$ MeV for the Vela pulsar. For example, the outwardly moving particles escape from the light cylinder with $\Gamma \sim 8 \cdot 10^6$ (for the Vela parameters). Thus, we expect that the calculated spectrum is improved between E_{min} and E_{out} .

The γ -rays radiated towards the star may be converted into e^\pm pairs by $\gamma B \rightarrow e^\pm B$ process and cause the pair-creation cascade. Cheng & Zhang (1999) showed that the synchrotron spectrum from these cascade pairs has the photon index of $p \sim 1.9$ in X -ray region. This spectral index is consistent with the pulsed *RXTE* soft component for the Vela pulsar (Harding et al. 2002). According to the model of Cheng et al. (2000), the γ -rays escaping from the gap through the *inner* boundary are much fainter than γ -rays through the *outer* boundary because the pair-creation occurs more efficiently near the inner boundary. In the present paper, the luminosity of the inwardly and the outwardly propagating γ -rays depend on the assumed currents j_1 and j_2 , respectively. In §4, we will find $j_1 \gg j_2$ to reproduce the observations. With this parameters, we have much more outwardly propagating γ -rays than inwardly.

The curvature of field lines will be different from that of dipole near the light cylinder. In this paper, therefore, we investigate the effect of the non-dipole field on the curvature spectrum; this effect was not considered in Hirotani et al. (2003). The many authors (e.g., Michel 1973; Contopoulos, Kazanas & Fendt 1999) have attempted to set the structure of the field lines, but it is yet far from an enough understanding of the actual structure of the magnetic field (e.g., non-aligned rotator with the pulsar wind). To examine the variation of the curvature radius of field line near to the light cylinder, we calculate each curvature spectrum for the following three configurations:

Case 1: the field line is defined by a pure dipole field that is tangent to the light cylinder (so-called the last-open field line for the dipole field);

Case 2: the field line is the same as Case 1 below $\varpi = 0.6\varpi_{lc}$, but deviates beyond $0.6\varpi_{lc}$ so that the radius of curvature may change as $R_c \propto 1/(1 - \varpi/\varpi_{lc})$;

Case 3: Below $0.6\varpi_{lc}$, the field line is defined by a pure dipole field that is tangent to the

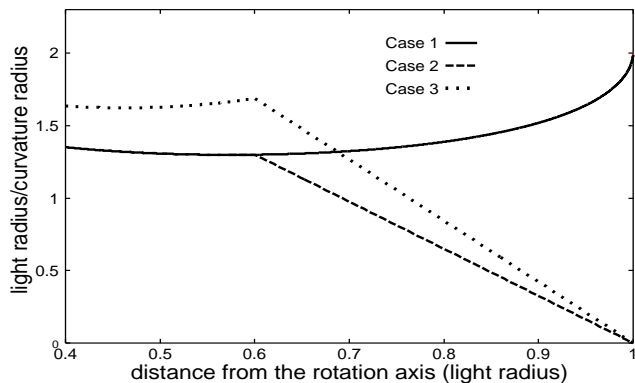


Figure 1. The curvature radius of last-open field line for three cases when $\alpha_{in}=45^\circ$. The solid, dashed-line and dotted-line correspond to the Case 1 (the case for pure dipole field), Case 2, and Case 3, respectively.

cylinder of radius $0.8\varpi_{lc}$. Beyond $0.6\varpi_{lc}$, the field line deviates from the pure dipole, and the radius of curvature of the field changes as $R_c \propto 1/(1 - \varpi/\varpi_{lc})$.

Case 2 and Case 3 simulate the effect of the increase of open magnetic fluxes. In Case 3, we take account of a possibility that the last-open field line changes inward dipole field line as compared with that of Case 1 by the influence of the pulsar wind or the electric current; for instance, the colatitude of the foot-point for the non-inclined pure dipole field line on the stellar surface is $\theta_f \sim (R_*/\varpi_{lc})^{1/2}$ for Case 1 (for Case 2) and $\theta_f \sim (R_*/0.8\varpi_{lc})^{1/2}$ for Case 3, where R_* is the star's radius. For the axisymmetric force-free magnetosphere, it is indicated that the field lines around the last-open field line deviate from dipole to radial configuration from $\varpi \sim 0.6\varpi_{lc}$, and have a point where $R_c = \infty$ near the light cylinder (e.g., fig. 3 in Contopoulos et al. 1999). These effects are simulated in Case 2 and Case 3. Fig. 1 shows the curvature field for Case 1 (solid-line), Case 2 (dashed-line), and Case 3 (dotted-line) between $\varpi = 0.4\varpi_{lc}$ and the light cylinder when the magnetic inclination α_{in} is 45° .

The electron-positron pairs produced by pair-creation will radiate by synchrotron process in the outside of the gap. These pairs are produced with significant pitch angle χ , and $\Gamma \sim 5 \cdot 10^3$. The critical photon energy of the synchrotron radiation around the outer-gap becomes

$$\begin{aligned}
 E_c &= \frac{3eh\Gamma^2 B}{4\pi m_e c} \sin \chi \\
 &= 4.4 \cdot 10^5 \left(\frac{\Gamma}{5 \cdot 10^3} \right)^2 \left(\frac{B}{10^6 \text{G}} \right) \sin \chi \text{ eV}.
 \end{aligned} \tag{28}$$

It is, therefore, entirely fair to neglect the synchrotron component emitted the outside of the gap when we consider a γ -ray spectrum above 100 MeV.

Table 1. The observed parameters

Pulsar	d kpc	Ω rad/s	B_{12} 10^{12}G	kT_s eV	A_s km^2
Vela	0.5	70.6	3.4	150	$6.6(d/0.5\text{kpc})^2$
B1706-44	1.8 (DM)/2.5 (H I)	61.6	3.1	143	$13(d/2.5\text{kpc})^2$

d is the distance from the earth to the pulsar. For PSR B1706-44, we adopt the 1.8 kpc proposed by dispersion measure and 2.5 kpc by H I absorption as the d . B_{12} represents the magnetic field strength at the star surface in units of 10^{12}G . The X -ray data are referred from Ögelman, Finley & Zimmerman (1993) for the Vela pulsar and Gotthelf et al. (2002) for PSR B1706-44.

4 APPLICATION

In this section we apply our model to the twin pulsars, PSR B0833-45 (Vela) and B1706-44, whose observed parameters are listed in Table 1. The model parameters are (j_{tot}, j_1, j_2) , the magnetic inclination angle α_{in} between the axes of rotation and magnetization, and the cross section area A_{gap} of the gap. The model parameters (j_{tot}, j_1, j_2) are chosen so as to reproduce the observed spectral properties. We adjust A_{gap} , which should not exceed $(\varpi_{lc})^2$, to the observed flux. For PSR B1706-44, the proposed distance to the pulsar is about 1.8 kpc by the dispersion measure and about 2.5 kpc by the H I absorption. The X -rays emission from PSR B1706-44 were reported for the first time by Gotthelf et al. (2002) with the *Chandra X-ray observatory*.

4.1 The electric structure

In Fig. 2, we present the calculated $E_{||}$ for Case 1 for both pulsars. The model parameters are $(j_{tot}, j_1, j_2) = (0.201, 0.191, 0.001)$ and $\alpha_{in} = 45^\circ$. The abscissa refers to the arc length from the pulsar surface along the last-open field line.

We see that the gap width $W_{||}$ is shorter than ϖ_{lc} , which is $4.25 \times 10^8\text{cm}$ for the Vela pulsar and $4.86 \times 10^8\text{cm}$ for PSR B1706-44. In the present model, $W_{||}$ is characterized by the mean free path for the pair-creation as Appendix A shows. Since the gap is filled with abundant γ -rays and X -rays, the mean-free path is shorter than ϖ_{lc} . The ratio of the mean-free path for the Vela pulsar and that for PSR B1706-44 becomes ~ 0.9 . As a result, we obtain the shorter gap width for the Vela pulsar (solid-line) than that for PSR B1706-44.

As Fig. 2 shows, a greater $E_{||}$ is obtained for the Vela pulsar than for PSR B1706-44. This can be understood from the fact that the strength of $E_{||}$ increase with $W_{||}$ and with the magnitude of ρ_{GJ} in the gap. The ratio of ρ_{GJ} for the Vela pulsar and that for PSR B1706-

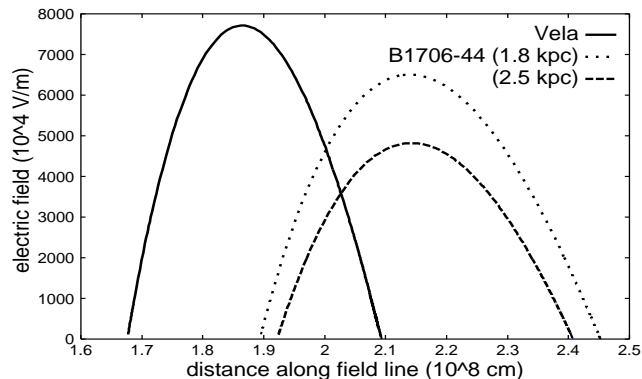


Figure 2. The acceleration field for the Vela pulsar (solid-line) and PSR B1706-44 (dotted-line for $d = 1.8$ kpc and dashed-line for $d = 2.5$ kpc). $(j_{tot}, j_1, j_2) = (0.201, 0.191, 0.001)$ and $\alpha_{in} = 45^\circ$

44 is ~ 2 . The effect of the difference in ρ_{GJ} overcomes that in the gap width, that is, PSR B1706-44 has a greater gap width $W_{||}$ than the Vela pulsar does.

Fig. 2 also shows how $E_{||}$ depends on the assumed distance for B1706-44. The gap width for $d = 1.8$ kpc (dotted-line) is wider than that for $d = 2.5$ kpc (dashed-line) because the X -ray luminosity decreases with decreasing assumed distance. The decreased X -ray photon density results in an increased pair-production mean-free path, and hence increased gap width. Therefore, if we adopt a nearer distance to the pulsar, the calculated $E_{||}$ becomes large as Fig. 2 shows. This also causes a harder spectrum in the case of $d = 1.8$ kpc than the case of $d = 2.5$ kpc (Fig. 4).

4.2 The γ -ray spectrum

The dimensionless current parameters are chosen so as to reproduce the observation. We obtain the best-fitting parameters $(j_{tot}, j_1, j_2) = (0.201, 0.191, 0.001)$ for the Vela pulsar with $\alpha_{in} = 45^\circ$. Fig. 3 shows the best-fitted curvature spectrum (solid-line) for outwardly propagating γ -rays, which is composed of radiation from the inside (dashed-line) and the outside (dotted-line) of the gap for Case 1. For comparison, we plot the phase averaged EGRET spectrum. It's peak and cut-off energies are in good agreement with the EGRET observations.

As we expected in §3, the spectrum from the outside of the gap appears between $E_{out} \sim 1$ GeV and $E_{min} \sim 80$ MeV with the photon index $p \sim 5/3$, where E_{out} and E_{min} correspond to the critical energy of curvature radiation of the particle's Lorentz factor at the boundary and the light cylinder, respectively. Below E_{min} , the spectrum has $p \sim 2/3$. By including the emission from outside of the gap, we can improve the spectrum above 100 MeV.

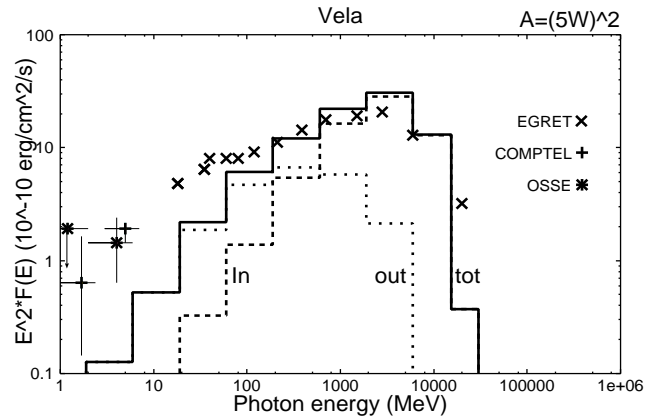


Figure 3. The calculated γ -rays spectrum for the Vela pulsar. The total spectrum (solid-line) includes the gap emission (dashed-line) and the emission from the outside of the gap (dotted-line). The model parameters are $(j_{tot}, j_1, j_2) = (0.201, 0.191, 0.01)$, $\alpha_{in} = 45^\circ$ and $A_{gap} = (5W_{||})^2$. The observed points are phase average spectra which are referred from Kanbach et al. (1994) for EGRET and Strickman et al. (1996) for OSSE and COMPTEL.

It follows from Fig. 3 that the calculated total spectrum in 100 MeV-GeV bands becomes slightly harder than the EGRET data. This is because we assume that the particle's motion is saturated at the equilibrium Lorentz factor (16), which overestimates the particle energy, and hence the γ -ray luminosity. A better predicted spectrum could be obtained if we would consider a unsaturated motion for the particles as Hirotani et al. (2003) did. Nevertheless the outside gap emission can also be treated properly with the Lorentz factor solved with equation (26).

Fig. 4 shows the *total* spectrum for PSR B1706-44. It is noteworthy that the same dimensionless parameters (j_{tot}, j_1, j_2) , and α_{in} as the Vela pulsar reproduce PSR B1706-44 data as well. However the observed peak energies for the two pulsars are different: About 3 GeV for the Vela pulsar, and about 1 GeV for PSR B1706-44. The difference is mainly due to the rotation periods. As showed in §4.1, the difference in ρ_{GJ} for the two pulsars appears as the difference of $E_{||}$. As a result, the saturated Lorentz factor given by equation (16) and the obtained spectral peak energy for PSR B1706-44 are less than those for the Vela pulsar. Thus, we need not change dimensionless parameters (j_{tot}, j_1, j_2) .

We fit the flux, by changing the cross section of the gap, A_{gap} . We use $A_{gap} = (5W_{||})^2 \sim (0.5\varpi_{lc})^2$ for the Vela pulsar, and $A_{gap} = (10W_{||})^2 \sim \varpi_{lc}^2$ for PSR B1706-44. The value of A_{gap} for B1706-44 appears to be too large, since the gap is located at $s \sim 0.5\varpi_{lc}$. In fact, we have $A_{gap}/4\pi(0.5\varpi_{lc})^2 \sim 1/3$ for B1706-44, which means that the hemisphere are almost covered with the gap. Such a large A_{gap} may be unrealistic. This flux problem will be discussed in §5.

Let us examine how the spectrum depends on the magnetic inclination, α_{in} . Romani &

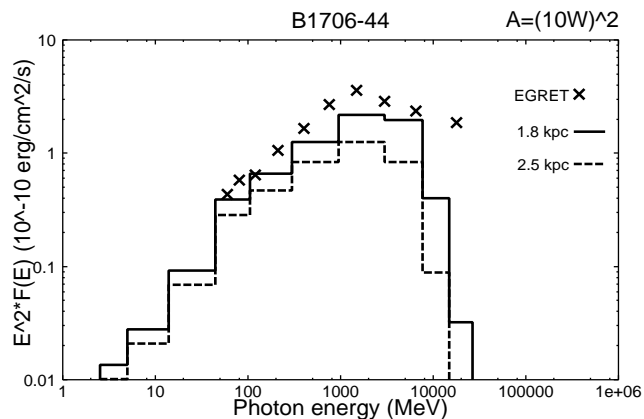


Figure 4. The calculated *total* γ -rays spectrum for PSR B1706-44. The solid-line, dashed-line represent the spectra for $d = 1.8$ kpc and $d = 2.5$ kpc. The model parameters are the same as in Fig. 3 except for $A_{gap} = (10W_{||})^2$. The observed points are referred from Thompson et al. (1996).

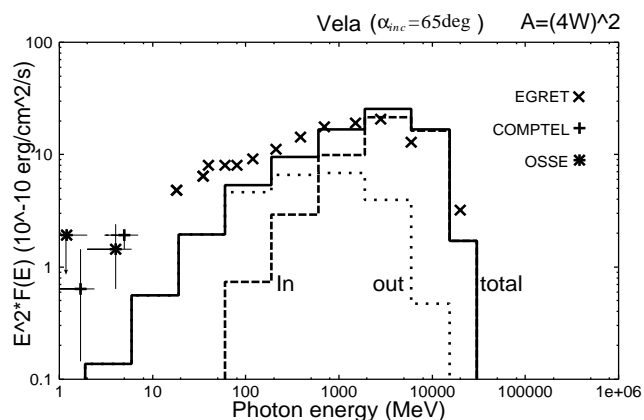


Figure 5. The same as Fig. 3 but for $\alpha_{in} = 65^\circ$. The current parameters are $(j_{tot}, j_1, j_2) = (0.202, 0.192, 0.02)$ and $A_{gap} = (4W_{||})^2$

Yadigaroglu (1995) estimated the inclination angle to be $\alpha_{in} \sim 65^\circ$ for the Vela pulsar and $\alpha_{in} \sim 45^\circ$ for PSR B1706-44 to explain the phase difference between the radio and γ -ray pulses. We also show the calculated spectrum in the case $\alpha_{in} = 65^\circ$ for the Vela pulsar in Fig. 5, where we adopt $(j_{tot}, j_1, j_2) = (0.202, 0.192, 0.002)$ to explain the observed spectral peak energy. The strength of magnetic field in the gap increase with α_{in} because the crossing point of the null surface and the last-open field line comes close to star. On the other hand, the gap width is shortened because the increased soft photon density results in the decreased pair-creation mean-free path for the inwardly propagating γ -rays. The former effect tends to increase $E_{||}$, while the latter to decrease it; therefore, the two effects compensate each other. As a result, we obtain the observed spectral peak energy by using almost the same current parameters for $\alpha_{in} = 45^\circ$. On these ground, we suggest that almost the same currents in unit of the GJ value are running through the gap for the Vela pulsar and PSR B1706-44.

4.3 Spectral dependence on the curvature of field line

Let us consider other configurations of the field line. Fig. 6 represents how the particle's Lorentz factor changes along the field lines with different field line configurations, where the Vela parameters are used. Three cases, Case 1 (solid), Case 2 (dashed) and Case 3 (dotted), are examined as had been described in §3. The Lorentz factors for Case 2 and Case 3 change little between $\varpi = 0.6\varpi_{lc}$ and ϖ_{lc} because of the stretched magnetic field lines.

Fig. 7 shows the calculated total spectra for the three cases. The dependence of each configuration of the field line appears in the spectra around 100 MeV. On such a stretched field line as in Case 2 or Case 3, curvature process little contributes to the spectrum. Because of the less efficient curvature emission, particles escape across the light cylinder with a large energy as compared with a pure dipole field. As a result, we obtain a greater lower-cut off energy $E_{min} \sim 200$ MeV for Case 2 (cf. $E_{min} \sim 80$ MeV for Case 1).

This effect is expected to appear in the observed spectra. Therefore, it is possible to diagnose at some level the actual field configuration in the magnetosphere from the observed spectra. For example, the EGRET, COMPTEL and OSSE observations indicate that the spectrum turns over below 100 MeV, that is, $E_{min} < 100$ MeV. Possibly a dipole-like field is preferable near the light cylinder than a stretched field, which is expected from magneto-hydrodynamics.

The effect of stretched fields will be manifest in a phase-resolved spectrum rather than a phase-averaged one. According to the double-peaked γ -ray models (e.g., Romani 1996; Cheng et al. 2000), the γ -ray photons radiated near the light cylinder contribute to the *first pulse-phase*, which leads the bridge-phase. Therefore, the stretching effect is expected to appear in the spectrum of the first pulse-phase. A diagnosis of the field line curvature is, therefore, carried out simultaneously with a position-pulse-phase mapping, which is necessary when we model the gap in a three-dimensional space. Thus, one can examine the field line geometry by using the fact that the curvature spectrum around 100 MeV depends on the field line geometry. On the other hand, in the phase-averaged spectrum, the radiation on stretching fields may be buried in the curvature radiation of low energy particles near the upper surface in the gap, where E_{\parallel} is small owing to the screening effect.

Even if a possible variation of the field line curvature is taken into account, the discrepancy in the COMPTEL and OSSE bands cannot be resolved. It seems difficult to diagnose the field line with these observations. In general, if the curvature radius varies smoothly on

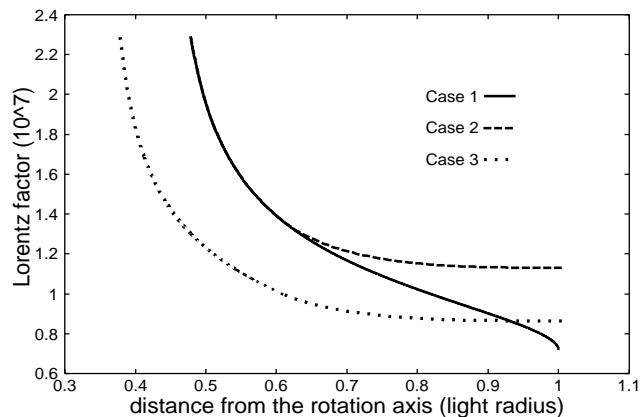


Figure 6. The development of the particle's Lorentz factor in the outside of the gap. The solid, dashed-line and dotted-line correspond to the Case 1, 2, and 3. The abscissa is the distance from the rotation axis in unit of ϖ_{lc} .

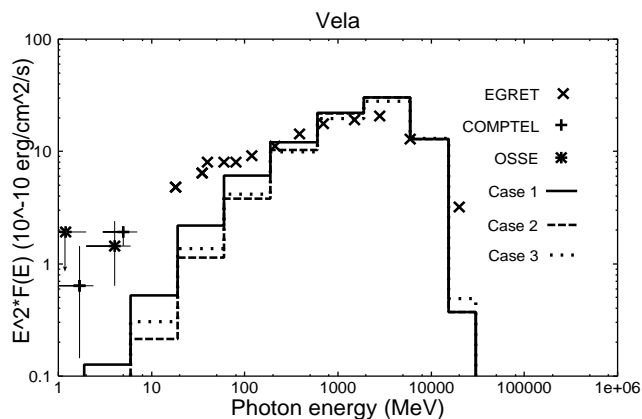


Figure 7. The calculated *total* γ -ray spectra for the Vela pulsar. The lines correspond to the same case as in Fig. 6. The cross section is chosen such that $A_{gap} = (5W_{||})^2$ for Case 1 and Case 2, $(4W_{||})^2$ for Case 3.

the particle's path to the light radius, we are able to think that the particles escape from the light cylinder with the Lorentz factor at which $ct_d \sim \varpi_{lc}$,

$$\Gamma_{lc} \sim 1.17 \times 10^7 \left(\frac{\Omega}{100\text{s}} \right)^{-1/3} \left(\frac{\langle R_c \rangle}{\varpi_{lc}} \right)^{2/3}, \quad (29)$$

where $\langle R_c \rangle$ is the averaged curvature radius of the field line along which the particles move. For this Lorentz factor and the radius of curvature, particles emit γ -rays at energies around

$$E_c^{lc} \sim 160 \left(\frac{\langle R_c \rangle}{\varpi_{lc}} \right) \text{ MeV}, \quad (30)$$

which may appear in the curvature spectrum as the lower energy cut-off E_{min} . If the observed break at ~ 10 MeV for the Vela pulsar were caused by this escape effect, we would have $\langle R_c \rangle \sim 0.1\varpi_{lc}$, which should be too short. On these ground, we conclude that the curvature radiation from the primary particles does not account for the COMPTEL and OSSE components.

5 DISCUSSION

In short, we showed that curvature flux emitted outside of the gap dominates that emitted within the gap around 100 MeV. With this correction, the model spectrum was improved above 100 MeV. We then found that the field line curvature near the light cylinder affects the curvature spectrum in several hundreds MeV. We also showed that the difference in spectral peak energies of the Vela pulsar and PSR B1706-44 is explained by intrinsic difference in the magnetospheric parameters of the individual pulsars. We need not change the dimensionless current parameters.

5.1 Dominance of j_1 to total current

In §4, we find that j_2 should be much smaller than j_1 . In this subsection, we consider the case in which j_2 is not smaller than j_1 . For a large inclination, (e.g., for α_{in} greater than or nearly equal to 45°), the gap width $W_{||}$ is mainly determined by the pair-creation mean-free path for the inwardly propagating γ -rays because the collision angle with X -rays is nearly head-on for the inwardly propagating γ -rays and nearly tail-on for the outwardly propagating γ -rays. In this case, $W_{||}$ sharply decreases with increase of j_2 . Because $E_{||}$ decreases with $W_{||}$, the spectrum becomes soft by increasing j_2 . Fig. 8 shows the spectra for $j_1 = 0.191$ and $j_g = 0.009$, and $j_2 = 0.001$ indicated by solid-line, but $j_2 = 0.021$ by dashed-line for the Vela pulsar. A choice of $j_2 = 0.021$, which is significantly larger than the best-fitting value but smaller than j_1 , does not reproduce the observed spectrum.

Although the cases of $j_1 < 0.1$ can reproduce the observed spectral peak by appropriately choosing j_2 , it is difficult to reproduce the observed flux with a cross section that is smaller than $(\varpi_{lc})^2$. Therefore, a large j_1 and a small j_2 are preferable.

5.2 Comparison with previous models

Romani (1996) discussed the γ -ray spectrum for the Vela pulsar by curvature radiation, assuming a specific energy distribution $dN_e/dE_{||} \propto E_{||}^{-1}$ to connect the assumed electric field, $E_{||} \propto 1/r$, and the number density of the particles at the upper surface of the gap. This relation gives the particle energy spectrum $dN_e/d\Gamma \propto \Gamma^{-4}$, which is identical with equation (27), as long as the particles have the saturated Lorentz factor (16). The curvature radiation of the *particles produced in the gap* dominates in the spectrum (see, fig. 5 in Romani 1996).

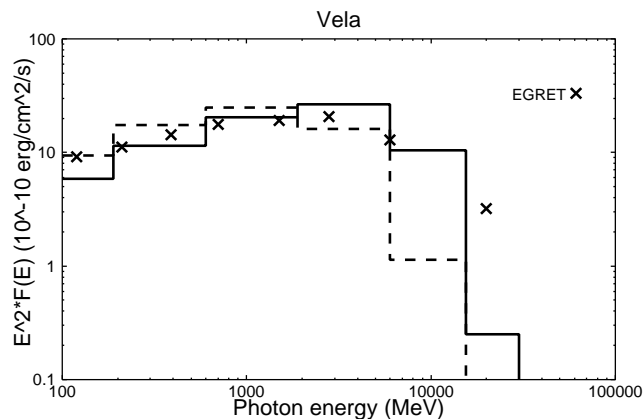


Figure 8. The γ -ray spectra for the Vela pulsar. The solid, dashed lines correspond to the spectra for $j_2=0.001$, 0.021 , respectively, when $j_1 = 0.191$, $j_g = 0.009$ and $\alpha_{in} = 45^\circ$. The cross section is chosen such that $A_{gap} = (5W_{||})^2$ for $j_2 = 0.001$ and $(7W_{||})^2$ for $j_2 = 0.021$

On the other hand, in the present model we obtained equation (27) as a result of the radiative loss of the particles in the outside of the gap. The pair flux produced in the gap is little, $j_g = 0.009$ for instance; therefore, the *injected particles* j_1 play a crucial role in the formation of the curvature spectrum above 100 MeV.

This difference in the origin of the γ -rays between the two models will come from the difference in geometrical picture of the gap, slab-like outer-gap model (Romani's picture) or thick gap model (present model). The slab-like gap model, the pioneering studies for which were done by Cheng et al. (1986a,b), assumes that the gap width along the magnetic field line is much larger than the trans-field thickness of the gap on the meridional plane. In this slab geometry, the number density of pairs near the upper surface of the gap grows exponentially in the trans-field direction by the pair-creation, because the γ -rays radiated in the gap can effectively cross the field lines before materializing as pairs. In the pair-creation region, because $E_{||}$ is not abruptly screened, a copious created particles are accelerated and emit the observable γ -rays.

In the present model, on the other hand, we assume that the gap width is much shorter than trans-field thickness. In this case, the radiated γ -rays do not effectively cross the field lines in the gap before materializing; therefore, we can consider the gap with the one-dimensional model. The calculated $E_{||}$ in this non-vacuum model decreases with increasing of pairs produced in the gap because of the screening effect. As a result, the cases of the large pair-flux production in the gap, the large j_{gap} in (22), do not reproduce the observed spectral peak around GeV. As discussed in §5.1, therefore, we give a large injected particle flux into the gap through a boundary with a small j_{gap} to explain the observations. If we consider

the Romani's picture within our electrodynamical treatment, we should deal with a model of two- or three-dimensional geometry because the present one-dimensional assumption can not be used for such slab-like geometry.

5.3 Three dimensional electrodynamical model

Although the difference in spectral shape of the twin pulsars, the Vela pulsar and PSR B1706-44, is explained with the same dimensionless current parameters, the difference in the flux is difficult to be understood. Because the two pulsars have almost the same magnetospheric parameters and the surface temperature, one may expect similar luminosities. If intrinsic luminosity were the same, difference in flux would be attribute to the distance so that the expected ratio of flux may be between 13 and 25. However, the observed value is about 5. Zhang and Cheng (1997) estimated the transverse thickness of the outer-gap by considering a condition for γ -rays to materialize marginally in photon-photon collisions, which may explain difference in A_{gap} between the two pulsars. They obtained

$$f \sim 5.5 P^{26/21} B_{12}^{-4/7} \quad (31)$$

where f is the transverse thickness in unit of the light radius, P is the rotational period. With this weak dependence on the magnetospheric parameters, one cannot expect difference in A_{gap} between the two pulsars. One possibility is difference in viewing angle. For this point, we cannot proceed without extending the present model to a three-dimensional one. We need to solve the trans-field structure of the electric field and the current distribution.

There is another limitation of the present one-dimensional approach. To get a reasonable spectrum, the dimensionless current is should be less than or nearly equal to 0.2 in units of the GJ value. Within the frame work of the one-dimensional model, this value cannot be enlarged because the gap is quenched by large currents. This fact limits the total luminosity seriously. On the other hand, a current of the order of the GJ value should circulate in the pulsar wind, and it is the current that runs through the gap on its way to the star and contributes to the spin-down. In the outer-gap model by Cheng et al. (1986a), pairs are created much in the convex side of the gap, and a large current is flowing there. To evaluate the net current in the gap and the resultant luminosity correctly, the trans-field structure must be taken into account.

Finally, we note that the present model can only be compared with the observed *phase-averaged* spectra. On the other hand, the *phase-resolved* spectra have been discussed with

three dimensional geometry such as Romani (1996) for the Vela pulsar and Cheng et al. (2000) for the Crab pulsar. We could discuss this issue from the electrodynamical point of view if we would extend the present approach into a three-dimensional model

REFERENCES

- Cheng K.S., Ho C., Ruderman M., 1986a, ApJ, 300, 500
Cheng K.S., Ho C., Ruderman M., 1986b, ApJ, 300, 522
Cheng K.S., Zhang L., 1999, ApJ, 515, 337
Cheng K.S., Ruderman M., Zhang L., 2000, ApJ, 537, 964
Contopoulos I., Kazanas D., Fendt. C., 1999, ApJ, 511, 351
Goldreich P., Julian W.H., 1969, ApJ, 157, 869
Gotthelf E.V., Halpern J.P., Dodson R., 2002, ApJ, 567, L125
Harding A.K., Strickman M.S., Gwinn C., Dodson R., Moffet D., McCulloch P., 2002, ApJ, 576, 376
Hirotani K., 2003, Progress in Astrophysics Researches, vol.1 (Nova Science), in press
Hirotani K., Shibata S., 1999, MNRAS, 308, 54
Hirotani K., Harding A.K., Shibata S., 2003, ApJ, 591, 334
Kanbach G., et al. 1994, A&A, 289, 855
Michel F.C., 1973, ApJ, 180, 207
Ögelman H., Finley J.P., Zimmerman H.U., 1993, Nat, 361, 136
Romani R.W., 1996, ApJ, 470, 469
Romani R.W., Yadigaroglu I.A., 1995, ApJ, 438, 314
Ruderman M.A., Sutherland P.G., 1975, ApJ, 196, 51
Strickman M.S., et al., 1996, ApJ, 460, 735
Sturrock P.A., 1971, ApJ, 164, 529
Thompson D.J., et al., 1996, ApJ, 465, 385
Thompson D.J., et al., 1999, ApJ, 516, 297
Zhang L., Cheng K.S., 1997, ApJ, 487, 370

APPENDIX A: THE ELECTRIC FIELD SCREENING AND THE GAP WIDTH

We give the gap width W_{\parallel} by solving the continuity equations (9), (12) with some approximations.

We integrate the Poisson equation (3) along the field line from s_1 to s_2 to obtain

$$\int_{s_1}^{s_2} [\rho(s) - \rho_{GJ}(s)] ds = 0, \quad (\text{A1})$$

namely, the total amount of the effective charge in the gap equals zero. For the case of the vacuum gap ($\rho = 0$), the null point, $\rho_{GJ} = 0$, is located between s_1 and s_2 . For a given s_1 , one can find s_2 so that (A1) may be satisfied. The gap width is arbitrary.

For a non-vacuum gap, W_{\parallel} is characterized by pair-creation mean-free path. Since the gap width is shorter than ϖ_{lc} (§4), we assume the physical quantities in the gap to be constant value except for the particle's number densities (N_{\pm}) and the distribution function (G_{\pm}) for γ -rays. Then equations (9) and (12) are combined to give

$$\frac{d^2 N_{\pm}(s)}{ds^2} = \pm[\alpha_+ N_+(s) - \alpha_- N_-(s)], \quad (\text{A2})$$

where

$$\alpha_{\pm} = \frac{1}{c^2} \int_0^{\infty} d\epsilon_{\gamma} \eta_{p\pm}(\epsilon_{\gamma}) \eta_c(\epsilon_{\gamma}). \quad (\text{A3})$$

With this solutions for $N_{\pm}(s)$ and the boundary conditions (20), (21), we obtain the following representation for the gap:

$$\begin{aligned} & \frac{\alpha_+ \alpha_- j_0 W_{\parallel}}{\sqrt{\alpha_+ + \alpha_-}} + \frac{\alpha_+ \left(j_2 - \frac{\alpha_+ j_0}{\alpha_+ + \alpha_-} \right) + \alpha_- \left(j_1 - \frac{\alpha_- j_0}{\alpha_+ + \alpha_-} \right)}{\sinh(\sqrt{\alpha_+ + \alpha_-} W_{\parallel})} \\ & + \frac{\alpha_+ \left(j_1 - \frac{\alpha_- j_0}{\alpha_+ + \alpha_-} \right) + \alpha_- \left(j_2 - \frac{\alpha_+ j_0}{\alpha_+ + \alpha_-} \right)}{\tanh(\sqrt{\alpha_+ + \alpha_-} W_{\parallel})} = 0. \end{aligned} \quad (\text{A4})$$

For a largely inclined pulsar (e.g. for α_{in} greater than or nearly equal to 45°), inwardly propagating γ -rays collide almost head-on with the surface blackbody X -rays. In contrast, outwardly propagating γ -rays collide almost tail-on. Due to this difference, we obtain

$$W_{\parallel} \sim \frac{c}{(f \eta_{p-} \eta_c \epsilon_{\gamma})^{1/2}} \cosh^{-1} \left(\frac{j_2 + j_g}{j_2} \right). \quad (\text{A5})$$

This equation indicates that W_{\parallel} for a large inclination is characterized by the pair-creation mean-free path of inwardly propagating γ -rays unless $j_2 = 0$.

By giving (j_{tot}, j_1, j_2) , the position of the gap in the pulsar magnetosphere is determined by the set of s_1 and s_2 that satisfies relation (A4) and condition (A1). Thus, it does not need to have the null point in the gap.